

How long do particles spend in vortical regions in turbulent flows?

Akshay Bhatnagar,^{1,2,*} Anupam Gupta,^{3,†} Dhruvadya Mitra,^{2,‡} Rahul Pandit,^{1,§} and Prasad Perlekar^{4,¶}

¹*Centre for Condensed Matter Theory, Department of Physics,
Indian Institute of Science, Bangalore 560012, India.*

²*Nordita, KTH Royal Institute of Technology and Stockholm University, Roslagstullsbacken 23, 10691 Stockholm, Sweden*

³*Laboratoire de Gnie Chimique, Universite de Toulouse, INPT-UPS, 31030, Toulouse, France.*

⁴*TIFR Centre for Interdisciplinary Sciences, 21 Brundavan Colony, Narsingi, Hyderabad 500075, India*

We obtain the probability distribution functions (PDFs) of the time that a Lagrangian tracer or a heavy inertial particle spends in vortical or strain-dominated regions of a turbulent flow, by carrying out direct numerical simulation (DNS) of such particles advected by statistically steady, homogeneous and isotropic turbulence in the forced, three-dimensional, incompressible Navier-Stokes equation. We use the two invariants, Q and R , of the velocity-gradient tensor to distinguish between vortical and strain-dominated regions of the flow and partition the $Q - R$ plane into four different regions depending on the topology of the flow; out of these four regions two correspond to vorticity-dominated regions of the flow and two correspond to strain-dominated ones. We obtain Q and R along the trajectories of tracers and heavy inertial particles and find out the time t_{pers} for which they remain in one of the four regions of the $Q - R$ plane. We find that the PDFs of t_{pers} display exponentially decaying tails for all four regions for tracers and heavy inertial particles. From these PDFs we extract characteristic time scales, which help us to quantify the time that such particles spend in vortical or strain-dominated regions of the flow.

PACS numbers: 47.27.-i, 47.55.Kf, 05.40.-a
Keywords: vortical regions; persistence time

I. INTRODUCTION

The characterization of the statistical properties of particles advected by a turbulent flow is a challenging problem. Not only is it of fundamental interest in fluid mechanics and non-equilibrium statistical mechanics, but it also has applications in geophysical fluid dynamics (e.g., raindrop formation in warm clouds [1–4]) and astrophysics (e.g., planet formation in astrophysical disks [5, 6]). An important challenge here is to obtain the time that such advected particles spend in vortical regions of the flow. We build on our studies of persistence-time statistics in two-dimensional (2D) fluid turbulence [7] to develop a natural way of defining a time for which a particle stays in a vortical region in the three-dimensional (3D) case. We illustrate how this is done for the case of statistically steady, homogeneous, and isotropic fluid turbulence by studying turbulent advection of (a) neutrally buoyant Lagrangian tracers (henceforth called tracers), which move with the fluid velocity at the particle, and (b) passive, heavy, inertial particles (henceforth heavy particles), which are spherical particles that are heavier than the carrier fluid and smaller than the Kolmogorov length scale η , at which viscous dissipation becomes significant. The trapping of a tracer into a vortical region is expected to give rise to very high values of particle ac-

celeration [8, 9]. The heavy particles are ejected from vortices [10–15] hence they are preferentially found in strain-dominated regions of the flow. This has been observed in direct numerical simulations (DNSs) by overlaying the positions of these particle on a pseudo-color plot of the magnitude of the vorticity, in a two-dimensional slice [16–18] through the simulation domain.

We estimate the time that a tracer or a heavy particle spends in a vortical or strain-dominated region of the flow by using the following, well-established technique for distinguishing between these flow regions [19–21]: At any point in the flow, the velocity-gradient matrix \mathcal{A} has two invariants Q and R [19, 20] (in the incompressible case, that we consider, the trace of \mathcal{A} is zero everywhere). Depending upon the signs of R and $\Delta = (27/4)R^2 + Q^3$, we can divide the $Q - R$ plane into four regions (Fig. 1); in two of these regions two eigenvalues of \mathcal{A} are complex conjugates of each other; and the topology of the local flow is vortical. The other two regions of the $Q - R$ plane corresponds to those points for which all the three eigenvalues of \mathcal{A} are real, and the local flow is strain-dominated. In our DNSs, we follow the trajectories of tracers or heavy particles in time and calculate the velocity-gradient matrix \mathcal{A} at the positions of these particles. The signs of R and Δ help us to identify whether a particle lies in a vortical or a strain-dominated region of the flow at a given instant of time. To obtain statistics for the time scales over which such particles stay in vortical or strain-dominated regions of the flow, it is natural to use the following idea of persistence from non-equilibrium statistical mechanics: For a fluctuating field ϕ , we find the probability distribution function (PDF) $P_\phi(t_{\text{pers}})$, which gives the probability that ϕ does not

*Electronic address: akshayphy@gmail.com

†Electronic address: anupam@physics.iisc.ernet.in

‡Electronic address: dhruva.mitra@gmail.com

§Electronic address: rahul@physics.iisc.ernet.in

¶Electronic address: perlekar@tifrh.res.in

change sign up to time t_{pers} . Persistence times can also be thought of as first-passage times [22].

Persistence has been studied in many non-equilibrium systems, e.g., the simple diffusion equation with random initial conditions [23], reaction-diffusion systems [24], and fluctuating interfaces [25]. In many systems it has been found that $P_\phi(t_{\text{pers}}) \sim t_{\text{pers}}^{-\theta}$, as $t_{\text{pers}} \rightarrow \infty$, where θ is called the persistence exponent [26]. This exponent θ can be universal; it can be obtained analytically only in a few cases; most often it is calculated numerically. We refer the reader to Refs. [26, 27] for reviews of such persistence problems.

In our DNS we calculate the PDF $P_\phi(t_{\text{pers}})$ of the times t_{pers} for which tracers or heavy particles remain in vortical or strain-dominated region. We find that, in the frame of tracers or heavy particles, these PDFs show exponentially decaying tails, from which we extract the decay times scales. Our study quantifies the dependence of these time scales on the Stokes number $\text{St} = \tau_p/\tau_\eta$, with τ_p the particle-response or Stokes time and τ_η the dissipation-scale time and provides, therefore, a natural way of answering the following question: How long do particles spend in vortical regions in turbulent flows?

The remainder of this paper is organized as follows. In Sec. II we present the 3D Navier-Stokes equation, the equations we use for the time evolution of tracers and heavy particles, and the numerical methods we use to solve these; in subsection II A we define the two invariants Q and R , which we use to distinguish between vortical and strain-dominated regions of the flow. Section III is devoted to a detailed description of our results; and Section IV contains concluding remarks.

II. MODEL AND NUMERICAL METHODS

We perform a DNS of the incompressible, three-dimensional, forced, Navier-Stokes (3D NS) equation

$$\partial_t \mathbf{u} + \mathbf{u} \cdot \nabla \mathbf{u} = \nu \nabla^2 \mathbf{u} - \nabla p + \mathbf{f}, \quad (1)$$

$$\nabla \cdot \mathbf{u} = 0, \quad (2)$$

where \mathbf{u} , p , \mathbf{f} , and ν are the velocity, pressure, force, and kinematic viscosity, respectively. Our simulation domain is a periodic box of length 2π . We solve the 3D NS equation by using the pseudo-spectral method with N^3 collocation points and the 2/3-dealiasing rule [28]. We use a constant-energy-injection forcing scheme [29], with a rate of energy injection ε . For time integration we use a second-order, exponential Adams–Bashforth scheme [30].

Heavy particles obey the following equations [31, 32]:

$$\begin{aligned} \dot{\mathbf{X}} &= \mathbf{V}, \\ \dot{\mathbf{V}} &= \frac{1}{\tau_p} [\mathbf{u}(\mathbf{X}) - \mathbf{V}], \end{aligned} \quad (3)$$

where \mathbf{X} and \mathbf{V} denote, respectively, the position and velocity of the particle, τ_p is the particle-response time,

TABLE I: Table of parameters for our DNS run with N^3 collocation points: ν is the kinematic viscosity, δt the time step, N_p is the number of tracers or heavy particles, k_{max} the largest wave number, ε the mean rate of energy dissipation; $\eta = (\nu^3/\varepsilon)^{1/4}$ and $\tau_\eta = (\nu/\varepsilon)^{1/4}$ are the dissipation length and time scales, respectively; $\lambda = \sqrt{2\nu E/\varepsilon}$ is the Taylor micro-scale, where E is the mean energy of the flow, and Re_λ is the Reynolds number based on λ , $I_l = \frac{\sum_k E(k)/k}{E}$ is integral length scale, where $E(k)$ is the energy spectrum of the flow, and $T_{eddy} = I_l/u_{rms}$ is the large eddy turn-over time, where u_{rms} is the root-mean-squared velocity of the flow.

N	ν	δt	N_p	Re_λ	$k_{max}\eta$
256	3.8×10^{-3}	5×10^{-4}	40,000	43	1.56
ε	η	λ	I_l	τ_η	T_{eddy}
0.49	1.82×10^{-2}	0.16	0.51	8.76×10^{-2}	0.49

$\mathbf{u}(\mathbf{X})$ is the flow velocity at the position \mathbf{X} , and dots denote time differentiation. We consider mono-disperse spherical particles, with radii $r_p \ll \eta$, material density ρ_p much greater than the fluid density ρ_f , and a small number density, so we neglect (a) the effect of the particles on the flow (i.e., we have passive particles) and (b) particle-particle interactions. We also assume that, as in several experiments, typical particle accelerations, in strongly turbulent flows, exceed significantly the acceleration because of gravity. We also study the statistics of tracers for which the equation of motion is

$$\dot{\mathbf{X}} = \mathbf{u}(\mathbf{X}). \quad (4)$$

We solve Eqs. (3) and (4) by using an Euler scheme in time to follow the trajectories of N_p particles in our DNS. The velocity-gradient matrix \mathcal{A} is calculated at each grid point by using spectral method. We use trilinear interpolation to calculate the components of $\mathbf{u}(\mathbf{X})$ and \mathcal{A} at the off-grid positions of the particles. Table II gives the list of parameters we use in our DNS.

A. $Q - R$ invariants of the velocity-gradient tensor

We follow Ref. [20] to note that the velocity-gradient matrix \mathcal{A} has three invariants under canonical transformations, namely, $P = \text{Tr}(\mathcal{A})$, $Q = -\text{Tr}(\mathcal{A}^2/2)$, and $R = -\text{Tr}(\mathcal{A}^3/3)$. Incompressibility yields $P = 0$, for all the points in our domain. The nature of the eigenvalues is determined by the signs of R and $\Delta = (27/4)R^2 + Q^3$, the discriminant of the characteristic equation of \mathcal{A} . This allows us to classify each point in our flow into four regions, in the $Q - R$ plane, as shown in Fig. 1. If Δ is large and positive, vorticity dominates the flow; if, in addition, $R < 0$ (Region B), vortices are compressed, whereas, if $R > 0$ (Region A), they are stretched. If Δ is large and negative, local strains are high and vortex formation is not favored; furthermore, if $R > 0$ (Region D), fluid elements experience axial strain, whereas, if $R < 0$ (Region

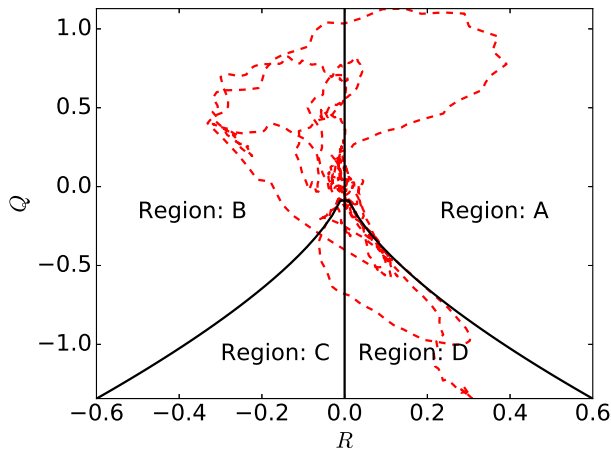


FIG. 1: (Color online) The flow is topologically different for values of Q and R that lie in the four regions shown in the $Q - R$ plane (after Ref. [20]); the black curve is the zero-discriminant line $\Delta = 0$. Regions A and B are vorticity-dominated regions; in region A vortices are stretched and in region B they are compressed. By contrast, regions C and D corresponds to strain-dominated or extensional regions; in region C fluid elements experience biaxial strain, whereas, in region D, they feel axial strain. The red dashed curve shows an illustrative path, in the $Q - R$ plane, as a tracer moves through the fluid in our DNS.

C), they feel biaxial strain [20].

III. RESULTS

From our simulations we find that the iso-surfaces of vorticity have tubular shapes that are well-known from DNSs of fully developed turbulence. The heavy particles distribute themselves away from regions of high vorticity.

We consider the motion of ten species of particles: tracers and nine heavy particles, with different values of St . We inject N_p particles of each species into the flow. We collect data for averages after the system of particles and the flow have reached a non-equilibrium, turbulent, but statistically steady, state. It has been already observed by over laying positions of heavy particles on two-dimensional contours of vorticity that the heavy particles distribute themselves away from regions of high vorticity. Here we look at a time-series of R and Δ obtained along the trajectory of a particle; a typical example of such a time series for a tracer is shown in Fig. (2). The intersection of any one of these curves with the black, horizontal line indicates the migration of a particle from one region of the $Q - R$ plane to another.

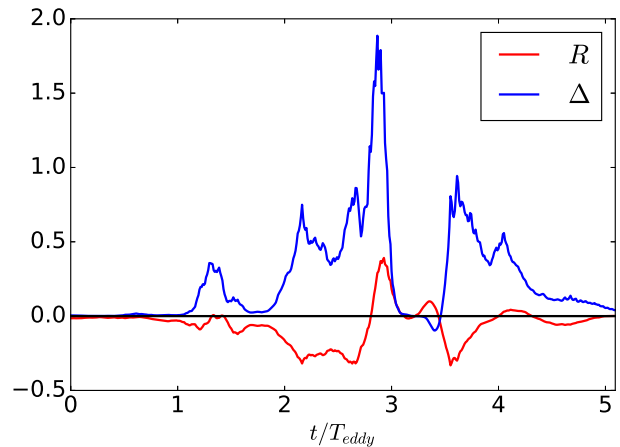


FIG. 2: (Color online) Plots of R (blue) and the discriminant Δ of the characteristic equation for the velocity-gradient tensor (green), calculated along the trajectory of a tracer as a function of the dimensionless time t/T_{eddy} . The intersection of any one of these curves with the black horizontal line indicates the migration of a particle from one region of the $Q - R$ plane to another. R and Δ are Nondimensionalized by Λ^3 and Λ^6 , respectively, where $\Lambda = u_\eta/\eta$.

A. Persistence times via Q and R

We follow the trajectory of each particle and calculate the components of \mathcal{A} and the values of Q and R at the particle position as a function of time. In Fig. 3 we plot contours of the joint PDFs of Q and R [$P(Q, R)$], on log scales; we calculate these values of Q and R along the trajectories of tracers and heavy particles, for different values of St . These joint PDFs show that the tracers are more likely to be in vorticity-dominated regions (region above the black curve in the $Q - R$ plane), as compared to the heavy particles; in addition, the probability of finding heavy particles in the vortical regions first decreases and then increases, as we increase St .

We obtain the PDFs from our DNS as follows: (A) In the Eulerian framework, by following the time evolution of Q and R at a fixed point (x, y, z) in space, we determine the time t_{pers} for which the flow at this point remains in one of the four regions described above; (B) in the Lagrangian framework we obtain the time t_{pers} for which a tracer resides in one of these regions; (C) the same calculation as in (B) but for heavy particles. For the Eulerian PDFs we use a superscript E, for tracer PDFs a superscript L, and for heavy-particle PDFs a superscript I. For each of the four regions in the $Q - R$ plane, we use the subscript A, B, C, and D. For example, P_A^I denotes the PDF of times t_{pers} that a heavy particle spends in the region A of the $Q - R$ plane.

In Fig. 4 we show semi-log plots of the PDFs of t_{pers} for the four regions A, B, C, and D, which indicate that these PDFs display exponentially decaying tails for large

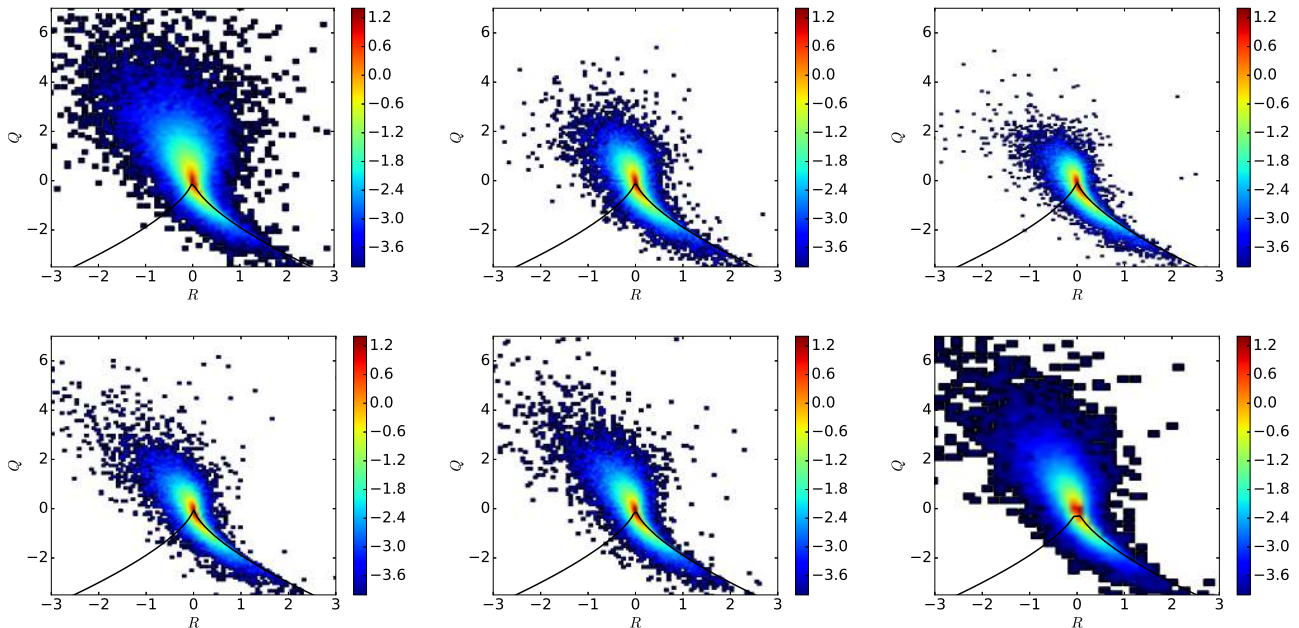


FIG. 3: (Color online) Contour plots of the joint PDFs of Q and R , on log scales, calculated along the trajectories of particles with different Stokes numbers, from top the left corner, (a) tracers, (b) $St = 0.1$, (c) $St = 0.5$, (d) $St = 1.0$, (e) $St = 1.4$, and (f) $St = 2.0$. Q and R are Nondimensionalized by Λ^2 and Λ^3 , respectively, where $\Lambda = u_\eta/\eta$. $\Delta = 0$ curve is shown by solid black line, $\Delta > 0$ corresponds to vorticity dominated region and $\Delta < 0$ corresponds to strain dominated region.

values of t_{pers} . We give the forms of these PDFs, for small values of t_{pers} , in the insets (lin-lin plots). We find that these PDFs do not go to zero as $t_{\text{pers}} \rightarrow 0$. The qualitative natures of these PDFs, for small t_{pers} , are similar for regions A, C, and D, but not for region B. These PDFs are obtained by computing the histograms and, therefore, they suffer from binning errors. To overcome these errors, we calculate the corresponding cumulative PDFs, by using the rank-order method [33]. We denote by Q_A^I the cumulative PDF (CPDF) that follows from P_A^I ; clearly,

$$P_A^I(t_{\text{pers}}) \equiv \frac{d}{dt_{\text{pers}}} Q_A^I(t_{\text{pers}}). \quad (5)$$

In Fig. 5 we give semi-log plots of $Q_A^I(t_{\text{pers}})$, for tracers and heavy particles, in regions A (top right), B (top left), C (bottom left), and D (bottom right). We observe that all these CPDFs have exponentially decaying tails, from which we extract the characteristic time scales T_α ($\alpha = A, B, C$, or D) that we list in Table II for all species of particles. We also note that, in regions A and B, which are vorticity dominated, T_A and T_B are largest for tracers; and they decrease as St increases. Furthermore, for all species of particles, $T_B > T_A$. The time scale T_C for region C, which is strain-dominated, does not change significantly with St . The time scale T_D for region D, where axial strain dominates, assumes its lowest value for tracers; and it changes only marginally as St increases.

To provide a clear answer to the question we pose in the title of this paper, we must calculate the PDFs of

the time t_{pers} for which heavy particles stay in vortical regions of the flow. We do this by monitoring the sign of Δ along the trajectories of the particles, for $\Delta > 0$ in vorticity-dominated regions of the flow and $\Delta < 0$ in strain-dominated ones. In Fig. 6 we shows the CPDFs t_{pers} for the cases where Δ remain positive (left panel) or negative (right panel), along the trajectories of tracers ($St = 0$) or heavy particles; we find that these CPDFs also have exponentially decaying tails. We extract the time scales T_{vortical} and T_{strain} , for particle residence in vortical or strain-dominated regions of the flow, respectively, by fitting exponential functions to these tails. We list these times in Table III for different values of St . We observe that T_{vortical} decreases monotonically as St increases, whereas T_{strain} first increases and then decrease. Furthermore, the values of T_{vortical} and T_{strain} indicate that tracers and heavy particles, with small values of St , stay longer in vortical regions of the flow than in strain-dominated ones, because the difference between T_{vortical} and T_{strain} is large here. By contrast, for heavy particles, with high values of St , the difference between T_{vortical} and T_{strain} is insignificant, so these particles spend roughly the same amount of time in vortical regions of the flow as in strain-dominated ones.

IV. CONCLUSIONS

Our DNS of tracers and heavy particles in statistically steady, homogeneous and isotropic turbulence in the

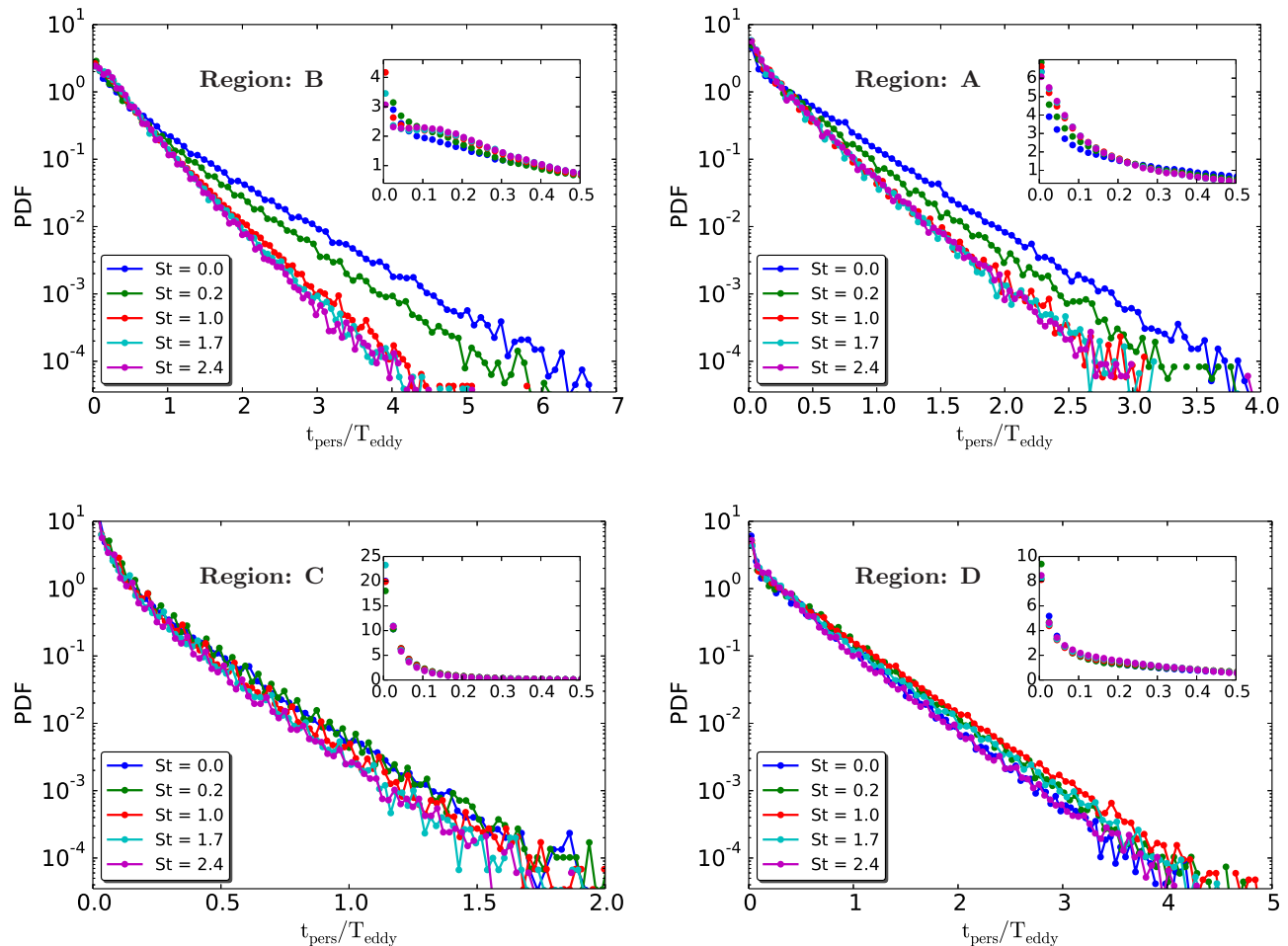


FIG. 4: (Color online) Semi-log plots of the persistence-time PDFs $P_\phi(t_{\text{pers}})$ of the times t_{pers} for the four regimes in the $Q - R$ plane, for different Stokes numbers; the inset shows $P_\phi(t_{\text{pers}})$ for small t_{pers} .

TABLE II: Values of characteristic time scales, T_α for all four regions of $Q - R$ plane ($\alpha = A, B, C, D$), calculated in the Eulerian frame for and in the frame of tracers and inertial particles, by fitting $Q_\alpha(t_{\text{pers}}/T_{\text{eddy}}) \sim \exp(-t_{\text{pers}}/T_\alpha)$ to the cumulative PDFs of residence time.

	T_A/T_{eddy}	T_B/T_{eddy}	T_C/T_{eddy}	T_D/T_{eddy}
Eulerian	0.13	0.23	0.08	0.13
Tracers	0.37	0.68	0.17	0.37
St = 0.1	0.35	0.63	0.18	0.39
St = 0.2	0.34	0.58	0.18	0.41
St = 0.5	0.34	0.48	0.18	0.42
St = 0.7	0.32	0.45	0.19	0.41
St = 1.0	0.32	0.44	0.19	0.42
St = 1.4	0.30	0.41	0.16	0.42
St = 1.7	0.29	0.39	0.16	0.41
St = 2.0	0.29	0.39	0.15	0.42
St = 2.4	0.28	0.37	0.16	0.39

forced, 3D NS equation has helped us to explore how long such particles spend in vortical regions of a turbulent flow and in strain-dominated ones by combining properties of the velocity-gradient tensor, which is well known in fluid mechanics, and the notion of persistence times, which has received considerable attention in non-equilibrium statistical mechanics. The Q and R invariants play a crucial role in our analysis of PDFs and CPDFs of persistence times, conditioned on the values of R and Δ . The exponential tails of these PDFs and CPDFs help us to extract time scales that we identify with particle-residence times in vortical or strain-dominated regions of the turbulent flow. We hope that our detailed study of persistence-time PDFs in 3D turbulent flows will lead to experimental studies of such statistics for tracers and heavy particles.

Our work is a natural generalization of a similar study for tracers [7] in two-dimensional, statistically steady, homogeneous and isotropic turbulent flows. In two-dimensions, instead of Q and R , we must use the Okubo-Weiss parameter $\Lambda \equiv \det(\mathcal{A})$. This study has found that

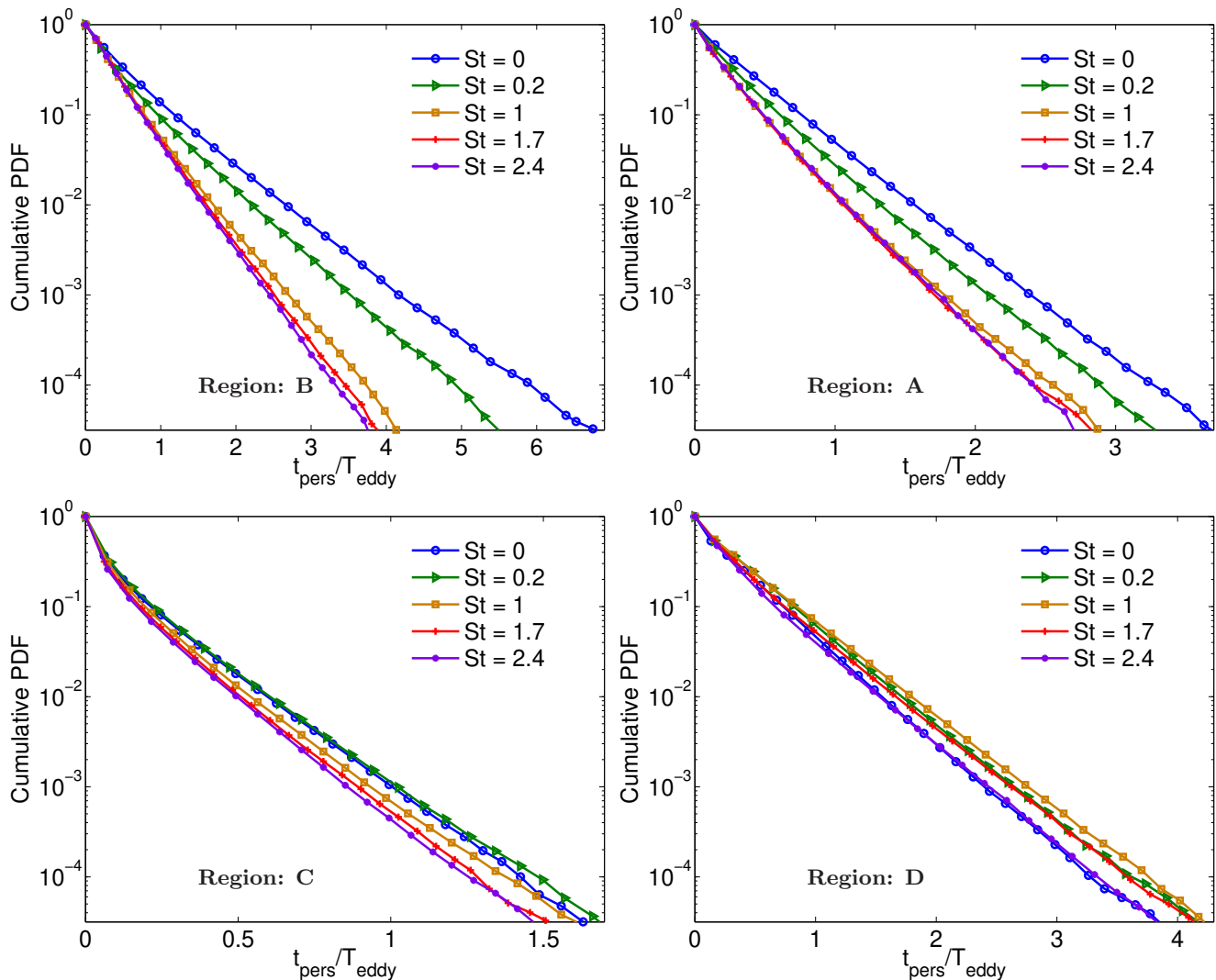


FIG. 5: (Color online) Semi-log plots of the cumulative persistence time PDFs (obtained by the rank-order method) for the four regimes in the $Q - R$ plane, for different values of the Stokes number.

TABLE III: Values of the characteristic time scales, for the vortical ($\Delta > 0$) and strain dominated ($\Delta < 0$) regions, calculated in the frame of tracers and heavy particles for different values of St .

	$T_{\text{vortical}}/T_{\text{eddy}}$	$T_{\text{strain}}/T_{\text{eddy}}$
Tracers	1.44	0.54
$St = 0.1$	1.11	0.59
$St = 0.2$	0.97	0.59
$St = 0.5$	0.73	0.62
$St = 0.7$	0.71	0.63
$St = 1.0$	0.64	0.60
$St = 1.4$	0.59	0.59
$St = 1.7$	0.56	0.57
$St = 2.0$	0.55	0.55
$St = 2.4$	0.55	0.51

the PDF of the persistence time τ , for a Lagrangian particle in vortical regions, displays a *power-law tail*, i.e., $P^\Lambda(\tau_-) \sim \tau_-^{-\theta}$, where the exponent $\theta \simeq 2.9$ [7]. By contrast, we show that the residence-time PDFs in 3D turbulent flows display exponentially decaying tails, for all species of particles and for all four regions in the $Q - R$ plane. The most likely reason for this qualitative difference of persistence-time PDFs (power-law as opposed to exponential tails) in 2D and 3D fluid turbulence is that, in the 3D case, the velocity-gradient tensor \mathcal{A} always has one real eigenvalue, so tracers and particles can escape more easily from vortical regions than they can in 2D turbulent flows. However, we must also note that the extent of the power-law region seen in the 2D study [7] increases with the Reynolds number. The Reynolds numbers that we can achieve in our 3D DNS is significantly lower than that in 2D. Therefore, very-high-resolution, large-Reynolds-number DNSs of 3D turbulence with trac-

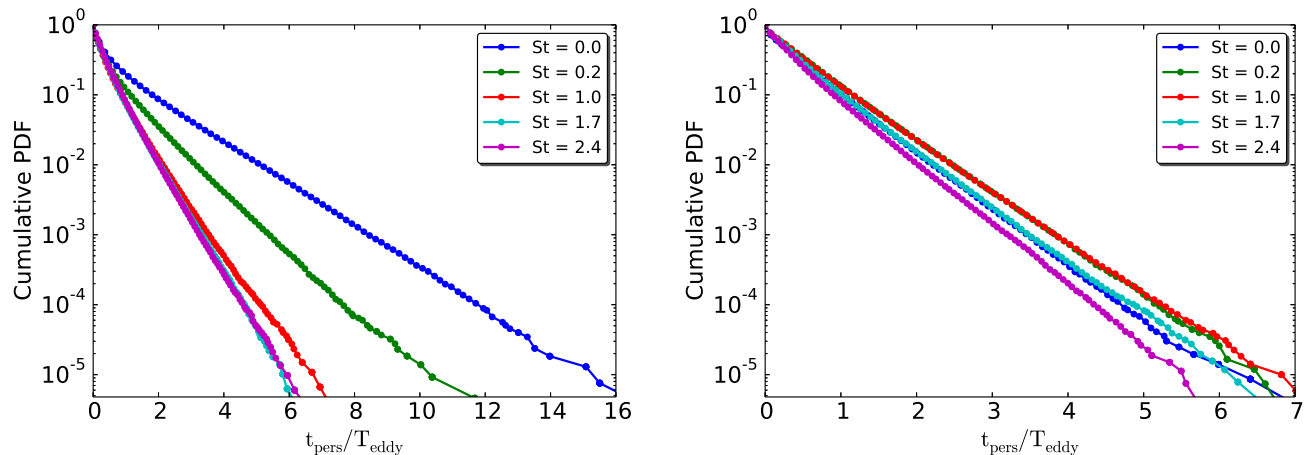


FIG. 6: (Color online) Semi-log plots of the cumulative persistence-time PDFs (obtained by the rank-order method) for vortical ($\Delta > 0$, left panel) and strain-dominated ($\Delta < 0$, right panel) regions, for different values of the Stokes number St (the plot for tracers is labeled by $St = 0$). From the slopes of the tails of these PDFs we extract the times T_{vortical} and T_{strain} , for particle residence in vortical or strain-dominated regions of the flow, respectively.

ers and particles are required to confirm the absence of power-law tails in persistence-time PDFs here.

The clustering of heavy particles in 3D fluid turbulence has been characterized by calculating a correlation dimension, which decreases first as St increases (for small St), thus indicating clustering; but this dimension reaches a minimum value near $St \simeq 0.7$, and then increases to a value $\simeq 3$ (i.e., a uniform distribution with insignificant clustering) as St increases beyond 0.7 [13]. This can be understood in terms of singularities (caustics) in the (particle) velocity gradient field, see e.g., Refs. [34, 35] for a review. The intuitive picture of clustering because of ejection from vortices is not enough to understand the clustering. Nevertheless, we observe by plotting the joint PDFs of Q and R as measured along the trajectories of heavy particles (Fig. 3): the probability of finding the heavy particles in the vortical regions first decreases and then increases, as we increase St . However, the characteristic time scales that we have calculated for such particles in vortical structures behave differently, insofar as they do not show such a clear, non-monotonic dependence on St (see Tables II and III).

Our DNS supports and quantifies the qualitative argument that heavy particles spend less time than tracers in vortical regions in 3D turbulent flows. However, the residence time scales depend only weakly on St , over the range we have in Tables II and III. Surprisingly, these characteristic time scales are comparable to the large-eddy turnover time. The values of these time scales can be used as input parameters in developing a model for the dynamics of the particles in turbulent flows. If the same characteristics time scales are calculated for Eulerian grid points, we find that they are about one-tenth of the large-eddy turnover time, i.e., they are of the same order as our Kolmogorov time scale. We see from the tails

of the cumulative PDFs in Fig. 6 that some of the particles can reside inside vortical regions for times that are much longer than T_{eddy} . Therefore, we need to run our DNSs for very long times to get good statistics. The results we present here have been obtained by running our DNSs for roughly $80T_{\text{eddy}}$. With such long runs, it is not possible to carry out very-high-resolution DNSs, at high Reynolds numbers and to obtain reliably the Reynolds-number dependence of persistence times.

One of the many longstanding questions in turbulence concerns the lifetime of vortices. Clearly, to measure the lifetime of a vortex we must have a precise definition of a vortex, which is, in itself, still controversial, (see, e.g., Ref. [36]). One of the several different criteria used to define a vortex, called the Q-criterion, is precisely the condition $\Delta > 0$ that we have used. If we use this condition to define a vortex, then the time a tracer particle spends in a vortex can be considered as a measure of the lifetime of a vortex itself. Therefore, with this interpretation, we have provided an answer to the old question: What is the typical lifetime of vortical structures? The cumulative probability distribution of the lifetime of a vortex, in homogeneous and isotropic turbulence, given in Fig. (6), has an exponential tail, which allows us to define a characteristic lifetime for a vortex; we give this lifetime in Table III. Other criteria for the definition of vortical regions can be used to measure the lifetime of vortices; and these may yield results that are different from those in Table III. An interesting attempt has been made to measure the PDF of the life time of vortical structures in Ref. [37] by using a DNS of light bubbles. This study lacked a precise definition of a vortex and had much smaller run times than those in our DNSs. Nevertheless, the characteristic lifetime of vortices, obtained in this study of Ref. [37], are roughly equal to those we

find.

An alternative way to define a vortical region (as opposed to a vortical point) is: “to be a compact region of vorticity, possibly unbounded in one direction, surrounded by irrotational fluid. Strictly speaking, the viscosity has to vanish for this definition to make sense, but we suppose that the viscosity is very small, and we allow transcendently small vorticity outside the vortex ...” (this quotation is from Ref. [38]). By using the lifetime of vortical regions, in a model for vortex tubes, Mori [39] has argued that the characteristic dimension of vortical regions increases as a power-law in time, with a universal exponent equal to $3/2$. As the Q-criteria is applicable to a point, but not to a region, we cannot comment on this result.

V. ACKNOWLEDGMENT

This work has been supported in part by Swedish Research Council under grant 2011-542 and 638-2013-9243

(DM), Knut and Alice Wallenberg Foundation (DM and AB) under project Bottlenecks for particle growth in turbulent aerosols (Dnr. KAW 2014.0048), and Council of Scientific and Industrial Research (CSIR), University Grants Commission (UGC), and Department of Science and Technology (DST India) (AB and RP). We thank SERC (IISc) for providing computational resources. PP and RP thank NORDITA for hospitality under their Particles in Turbulence program; DM thanks the Indian Institute of Science for hospitality during the time some of these calculations were initiated.

-
- [1] R. A. Shaw, Annual Review of Fluid Mechanics **35**, 183 (2003).
 - [2] W. W. Grabowski and L.-P. Wang, Annual Review of Fluid Mechanics **45**, 293 (2013).
 - [3] M. Pinsky and A. Khain, Journal of aerosol science **28**, 1177 (1997).
 - [4] G. Falkovich, A. Fouxon, and M. Stepanov, Nature **419**, 151 (2002).
 - [5] P. J. Armitage, Astrophysics of Planet Formation (Cambridge University Press, Cambridge, UK, 2010).
 - [6] I. De Pater and J. J. Lissauer, Planetary sciences (Cambridge University Press, ADDRESS, 2015).
 - [7] P. Perlekar, S. S. Ray, D. Mitra, and R. Pandit, Physical review letters **106**, 054501 (2011).
 - [8] F. Toschi *et al.*, Journal of Turbulence N15 (2005).
 - [9] L. Biferale and F. Toschi, Journal of Turbulence N40 (2005).
 - [10] J. K. Eaton and J. Fessler, International Journal of Multiphase Flow **20**, 169 (1994).
 - [11] L. R. Collins and A. Keswani, New Journal of Physics **6**, 119 (2004).
 - [12] H. Yoshimoto and S. Goto, Journal of Fluid Mechanics **577**, 275 (2007).
 - [13] J. Bec *et al.*, Physical review letters **98**, 084502 (2007).
 - [14] L. Biferale *et al.*, Physics of Fluids (1994-present) **17**, 115101 (2005).
 - [15] M. R. Maxey, Journal of Fluid Mechanics **174**, 441 (1987).
 - [16] L. Biferale *et al.*, Progress in Turbulence II (Springer, ADDRESS, 2007), pp. 207–212.
 - [17] J. Bec, H. Homann, and S. S. Ray, Physical review letters **112**, 184501 (2014).
 - [18] M. Cencini *et al.*, Journal of Turbulence N36 (2006).
 - [19] M. Chong, A. E. Perry, and B. Cantwell, Physics of Fluids A: Fluid Dynamics (1989-1993) **2**, 765 (1990).
 - [20] B. J. Cantwell, Physics of Fluids A: Fluid Dynamics (1989-1993) **5**, 2008 (1993).
 - [21] A. Perry and M. Chong, Annual Review of Fluid Mechanics **19**, 125 (1987).
 - [22] S. Redner, A guide to first-passage processes (Cambridge University Press, ADDRESS, 2001).
 - [23] S. N. Majumdar and C. Sire, Physical review letters **77**, 1420 (1996).
 - [24] E. Ben-Naim, Physical Review E **53**, 1566 (1996).
 - [25] J. Krug *et al.*, Physical Review E **56**, 2702 (1997).
 - [26] A. J. Bray, S. N. Majumdar, and G. Schehr, Advances in Physics **62**, 225 (2013).
 - [27] S. N. Majumdar, Current Science **77**, (1999).
 - [28] C. Canuto, M. Y. Hussaini, A. Quarteroni, and T. A. Zang, Spectral methods in fluid dynamics (PUBLISHER, ADDRESS, 1988).
 - [29] G. Sahoo, P. Perlekar, and R. Pandit, New Journal of Physics **13**, 013036 (2011).
 - [30] A. Bhatnagar, Ph.D. thesis, Indian Institute of Science Bangalore, 2016, unpublished thesis.
 - [31] R. Gatignol, Journal de Mécanique théorique et appliquée **2**, 143 (1983).
 - [32] M. R. Maxey and J. J. Riley, Physics of Fluids (1958-1988) **26**, 883 (1983).
 - [33] D. Mitra, J. Bec, R. Pandit, and U. Frisch, Phys. Rev. Lett **94**, 194501 (2005).
 - [34] A. Pumir and M. Wilkinson, arXiv preprint arXiv:1508.01538 (2015).
 - [35] K. Gustavsson and B. Mehlig, Advances in Physics **65**, 1 (2016).
 - [36] J. Jeong and F. Hussain, Journal of fluid mechanics **285**, 69 (1995).
 - [37] L. Biferale, A. Scagliarini, and F. Toschi, Physics of Fluids **22**, 065101 (2010).
 - [38] D. Pullin and P. Saffman, Annual review of fluid mechanics **30**, 31 (1998).
 - [39] H. Mori, Progress of theoretical physics **65**, 1085 (1981).